

# Perfect Reconstruction Conditions and Design of Oversampled DFT-Modulated Transmultiplexers

Cyrille Siclet,<sup>1</sup> Pierre Siohan,<sup>2</sup> and Didier Pinchon<sup>3</sup>

<sup>1</sup>Laboratoire des Images et des Signaux (LIS), Université Joseph Fourier, 38402 Saint Martin d'Hères Cedex, France

<sup>2</sup>Laboratoire RESA/BWA, Division Recherche et Développement, France Télécom, 4 rue du Clos Courtel, 35512 Cesson Sévigné Cedex, France

<sup>3</sup>Laboratoire Mathématiques pour l'Industrie et la Physique (MIP), Université Paul Sabatier, Toulouse 3, 31062 Toulouse Cedex 9, France

Received 1 September 2004; Revised 12 July 2005; Accepted 19 July 2005

This paper presents a theoretical analysis of oversampled complex modulated transmultiplexers. The perfect reconstruction (PR) conditions are established in the polyphase domain for a pair of biorthogonal prototype filters. A decomposition theorem is proposed that allows it to split the initial system of PR equations, that can be huge, into small independent subsystems of equations. In the orthogonal case, it is shown that these subsystems can be solved thanks to an appropriate angular parametrization. This parametrization is efficiently exploited afterwards, using the compact representation we recently introduced for critically decimated modulated filter banks. Two design criteria, the out-of-band energy minimization and the time-frequency localization maximization, are examined. It is shown, with various design examples, that this approach allows the design of oversampled modulated transmultiplexers, or filter banks with a thousand carriers, or subbands, for rational oversampling ratios corresponding to low redundancies. Some simulation results, obtained for a transmission over a flat fading channel, also show that, compared to the conventional OFDM, these designs may reduce the mean square error.

Copyright © 2006 Cyrille Siclet et al. This is an open access article distributed under the Creative Commons Attribution License, which permits unrestricted use, distribution, and reproduction in any medium, provided the original work is properly cited.

## 1. INTRODUCTION

Since the mid-nineties, oversampled filter banks have received a considerable amount of attention. Originally, most of the studies were devoted to subband encoder structures corresponding to a serial concatenation of an analysis and synthesis filter bank having a decimation and expansion factor inferior to the number of filters [1]. In this paper, as in [2–6], we are mainly interested in the converse situation, which corresponds to a transmultiplexer where the transmitter is composed of a synthesis filter bank (SFB) generating the transmitted signal that is afterwards estimated by a receiver composed of an analysis filter bank (AFB). Oversampling then means that the expansion and decimation ratios have to be higher than the number of subbands in order to get a perfect estimation of the transmitted symbols, that is, the equivalent of the perfect reconstruction (PR) conditions used in the filter bank context.

In general, in the oversampled case, a duality relationship between filter banks and transmultiplexers, such as the one proved in [7] for critically decimated systems, does not exist. However, if we restrict ourselves to the class of oversampled

filter banks using an exponential modulation based on the discrete Fourier transform (DFT), under certain conditions, duality relations can still be established. As in [2, 3], in the orthogonal case, they may be proved showing the equivalence of the PR conditions. They can also appear in a more general setting as a consequence of the duality between frames and biorthogonal families in the Weyl-Heisenberg (Gabor) systems theory, see [8] and references therein. This duality naturally gives a more general impact to the family of oversampled DFT-modulated filter banks.

In a transmission context, oversampled DFT-modulated filter banks can be seen as a discrete-time approach to get efficient multicarrier transmission systems. In this field, for the time being, the reference is still the orthogonal frequency division multiplex (OFDM), also known as the discrete multitone (DMT) for wired transmission. Indeed, OFDM/DMT is now part of various transmission standards related to wireless and wired links. Nevertheless, OFDM presents some weaknesses which explain why several studies are still undertaken to propose efficient alternatives. OFDM corresponds to a critically decimated DFT-modulated filter bank, therefore it cannot have a good frequency localization [9]. This

directly leads to one of the main drawbacks of the conventional OFDM with DFT filters whose attenuation is approximately limited to the 13 dB provided by a rectangular window shaping. Higher attenuation levels are desirable as illustrated, for example, in [10] in the case of transmission over very high-bit-rate digital subscriber lines (VDSL). Depending on the application at hand, they may be required at the transmitter, to limit the out-of-band energy, and/or at the receiver for combatting narrowband interference or frequency shifts between the transmitter and the receiver. On the other hand, it is now widely recognized that time-frequency localization is an essential feature for transmission over time-frequency dispersive channels.

A first alternative to introduce an efficient pulse shaping is based on a variant of OFDM where the modulation of each carrier is properly modified. Instead of using a classical quadrature amplitude modulation (QAM), each carrier is modulated using a staggered offset QAM (OOQAM), leading to a modulation now known as OFDM/OQAM. In theory, OFDM/OQAM allows it to get a maximum spectral efficiency. Recently, there were several proposals elaborated either using continuous-time [11–13] or discrete-time [14, 15] formalisms, some of these orthogonal schemes are generalized afterwards to get biorthogonal modulation, that is, BFDM/OQAM [8, 16]. But then, the introduction of an offset complicates the channel estimation task.

Another alternative in order to introduce pulse shaping, the one developed in the present paper, is to build oversampled multicarrier systems. Then, channel estimation becomes easier, but on the other hand, oversampling also means added redundancy, and consequently loss of spectral efficiency. For instance, to be competitive with existing systems, oversampled transmultiplexers must not add more redundancy than that introduced in a conventional OFDM system with the cyclic prefix, that is, an extension of the symbol duration that generally only corresponds to a small fraction of the overall useful symbol time duration. Furthermore, as multicarrier systems often require a high (hundreds) or a very high (thousands) number of carriers, we need a design method that satisfies both requirements. Several approaches have been proposed to provide appropriate answers to these problems. They can again be classified according to the type of formalism, continuous-time or discrete-time, which is used to get the desired pulse shapes. References [8, 17–19] share a common feature that is to propose prototype functions for Weyl-Heisenberg (or Gabor) systems with good time-frequency localization. Furthermore in [18, 19], optimization of the pulse shapes is carried out with respect to characteristic parameters of the time-frequency dispersive channels. However, even if in [18] the authors reach a high spectral efficiency, with an oversampling ratio (or a redundancy) of 5/4, it is for a system with only 64 carriers. As in [2, 3], and more recently in [6], our own approach, contrary to [17–19], is to use a discrete-time formalism with finite impulse response (FIR) causal filters, and we take the reconstruction delay into account. We then get oversampled filter banks that can be directly implemented without a loss of the

desired properties: frequency selectivity or time-frequency localization. Thus, in this paper, we focus on the case of oversampled modulated transmultiplexers. Similarly with [2, 3], for transmultiplexers, or [1, 20] for filter banks, we use a DFT modulation. This means that in the SFB and AFB, all filters can be obtained by means of a multiplication of a prototype filter by a complex exponential, thus allowing efficient fast implementations afterwards. With this approach, the design of spectrally efficient multicarrier systems with a high number of carriers becomes possible, which can be seen in [3], but more particularly in [5, 21]. This is not the case when considering a more general filter bank structure [4]. However, even if for the DFT-modulated filter banks, the design is reduced to one, as in [2, 3], or two [6] prototype filters, it remains difficult to get systems with high number of carriers and low oversampling ratios. In [2, 3], the results presented for orthogonal systems are limited to 32 carriers and an oversampling ratio equal to 3/2. In [6], the authors optimize a biorthogonal transmultiplexer with 80 subcarriers and a higher spectral efficiency, with an oversampling ratio equal to 5/4. In this paper, we describe the different steps of an approach that recently allowed us to obtain design results for a similar sampling ratio but a far larger number of carriers.

In particular, we investigate

- (i) the necessary and sufficient PR conditions, expressed with respect to the polyphase components of the prototype filters related to oversampled BFDM/QAM systems or, equivalently, to oversampled DFT filter banks;
- (ii) a simplification of the above result, with a splitting of the large initial set of PR equations into a less large set of small independent subsystems and the proof that in a first step, only small subsystems have to be solved;
- (iii) an approach which allows orthogonal systems using FIR filters to represent the solutions of each subsystem thanks to angular parameters;
- (iv) the application to oversampled DFT transmultiplexers of the compact representation approach, proposed in [22], for critically decimated filter banks;
- (v) a comparison between conventional and oversampled OFDM in the case of a transmission over a frequency dispersive channel.

Our paper is organized as follows. In Section 2, we present the general features concerning the oversampled DFT-modulated transmultiplexer, its polyphase decomposition, and its input-output relation. In Section 3, we provide the PR conditions for the biorthogonal systems and a decomposition technique to get independent subsets of the PR conditions. The parametrization, initially presented in [21], is summarized in Section 4. In Section 5, we recall the basic principle of the compact representation method and present design results, using two different optimization criteria: out-of-band energy and time-frequency localization. Finally, Section 6 is devoted to the presentation of our comparison between conventional and oversampled OFDM in a transmission context.

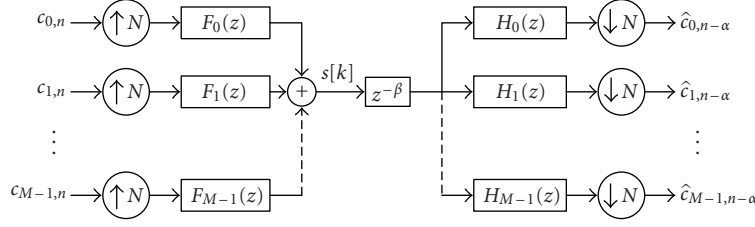


FIGURE 1: Oversampled BFDM/QAM transmultiplexer.

### Notations

$\mathbb{Z}$ ,  $\mathbb{C}$  denote the set of integers and complex numbers, respectively.  $l_2(\mathbb{Z})$  corresponds to the space of square-summable discrete-time sequences. Vectors and matrices are denoted with bold italic letters, for instance  $\mathbf{E}$ . We denote discrete filters of  $l_2(\mathbb{Z})$  with lowercase letters, for instance  $h[n]$ , and their  $z$ -transform with uppercase letters, such as  $H(z)$ . Superscript  $*$  denotes complex conjugation. For a filter  $H(z)$ ,  $H^*(z) = \sum_n h[n]^* z^{-n}$ . The tilde notation  $\tilde{\cdot}$  denotes paraconjugation:  $\tilde{H}(z) = H^*(z^{-1})$ .  $\langle \cdot, \cdot \rangle$  is the classical inner product of  $l_2(\mathbb{Z})$ :  $\langle x, y \rangle = \sum_{k \in \mathbb{Z}} x^*[k]y[k]$ . For  $M$  and  $N$  two integer parameters,  $\text{lcm}(M, N)$  and  $\text{gcd}(M, N)$  designate the lowest common multiple and the greatest common divisor of  $M$  and  $N$ , respectively. Lastly,  $\delta_{m,n}$  denotes the Kronecker operator and for any real-valued parameter  $x$ ,  $[x]$  is the integer part of  $x$ .

## 2. OVERSAMPLED DFT-MODULATED TRANSMULTIPLEXERS

The purpose of this section is to provide a brief presentation of oversampled DFT-modulated transmultiplexers, and to derive the transfer matrix of the overall system, based on a polyphase decomposition. We consider FIR causal filters and we take the reconstruction delay into account.

### 2.1. General presentation

Oversampled DFT-modulated transmultiplexers are a particular type of transmultiplexers for which synthesis filters and analysis filters are obtained thanks to a DFT modulation of a unique synthesis filter and a unique analysis filter. Thus, considering an  $M$ -band DFT-modulated transmultiplexer and for  $0 \leq m \leq M-1$ , the impulse responses of the FIR synthesis and analysis filters  $F_m(z)$  and  $H_m(z)$  are given by

$$\begin{aligned} f_m[k] &= f[k]e^{j(2\pi/M)m(k-D/2)}, & 0 \leq k \leq L_f - 1, \\ h_m[k] &= h[k]e^{j(2\pi/M)m(k-D/2)}, & 0 \leq k \leq L_h - 1, \end{aligned} \quad (1)$$

respectively.  $D$  is an integer parameter related to the reconstruction delay and  $f[k]$ ,  $h[k]$  are the impulse responses of the synthesis and analysis prototype filters  $F(z)$  and  $H(z)$ , respectively.

It can be shown [16] that a delay has to be introduced along the transmission channel, just before the demodulation stage, in order to perfectly correspond to an oversampled BFDM/QAM modulation. Denoting this transmission delay by  $\beta$  with

$$D = \alpha N - \beta, \quad 0 \leq \beta \leq N - 1, \quad (2)$$

it appears that the reconstruction delay is equal to  $\alpha$  samples. Thus, a discrete-time oversampled BFDM/QAM system with  $M$  carriers and an oversampling ratio  $r = N/M \geq 1$  is equivalent to the transmultiplexer depicted in Figure 1. In this figure, we denote by  $c_{m,n}$  and  $\hat{c}_{m,n}$  ( $0 \leq m \leq M-1$ ,  $n \in \mathbb{Z}$ ) the QAM symbols we want to transmit and the QAM symbols we receive after demodulation, respectively.

### 2.2. Polyphase approach

As is the case for filter banks [20, 23], the polyphase approach is also a natural tool to describe the transmultiplexer. Setting  $\omega = e^{-j(2\pi/M)}$ , we can write its synthesis and analysis filters  $F_m(z) = \omega^{m(D/2)}F(z\omega^m)$  and  $H_m(z) = \omega^{m(D/2)}H(z\omega^m)$ , respectively. Let us also define the integer parameters  $M_0$  and  $N_0$  by  $M_0N = MN_0 = \text{lcm}(M, N)$ . Then, as in [3, 20], we rewrite  $F_m(z)$  and  $H_m(z)$  using their  $M_0N$  type-I polyphase components [24]:

$$\begin{aligned} F_m(z) &= \sum_{l=0}^{M_0N-1} z^{-l}F_{l,m}(z^{M_0N}), \\ H_m(z) &= \sum_{l=0}^{M_0N-1} z^{-l}H_{m,l}(z^{M_0N}). \end{aligned} \quad (3)$$

Denoting by  $\mathbf{F}_p(z)$  and  $\mathbf{H}_p(z)$  the  $M_0N \times M$  and  $M \times M_0N$  polyphase matrices, respectively, defined by  $[\mathbf{F}_p]_{l,m}(z) = F_{l,m}(z)$  and  $[\mathbf{H}_p]_{m,l}(z) = H_{m,l}(z)$ , and using noble identities [24], we finally get the equivalent scheme depicted in Figure 2, where  $C_m(z)$  and  $\hat{C}_m(z)$  are the  $z$ -transforms of  $c_{m,n}$  and  $\hat{c}_{m,n}$ ,  $0 \leq m \leq M-1$ , respectively. Thus, even if it is less obvious [18], a polyphase implementation is possible even for noninteger oversampling ratios. Moreover, it is worthwhile mentioning that this scheme has various fast algorithm implementations using fast Fourier transforms or inverse fast Fourier transforms [16].

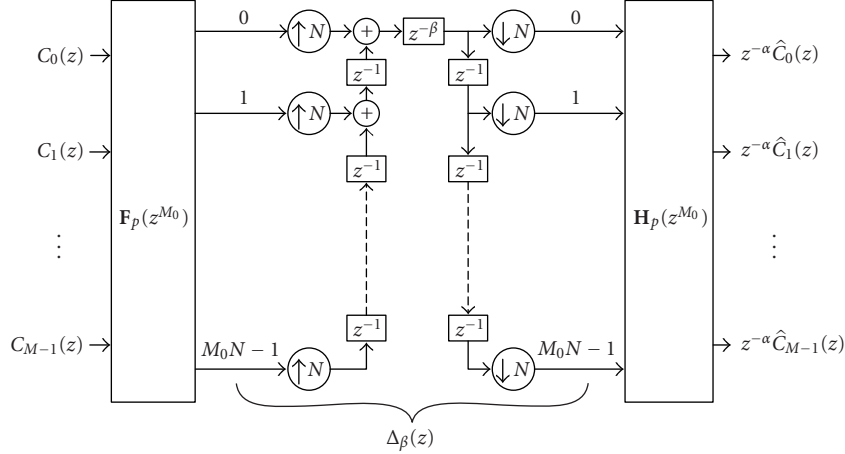


FIGURE 2: BFDM/QAM transmultiplexer with a simplified polyphase implementation.

### 2.3. Input-output relations

The transfer matrix  $\mathbf{T}(z)$  of the transmultiplexer is defined by  $\hat{\mathbf{C}}(z) = \mathbf{T}(z)\mathbf{C}(z)$ , where  $\mathbf{C}(z)$  and  $\hat{\mathbf{C}}(z)$  are two column vectors with entries  $C_m(z)$  and  $\hat{C}_m(z)$ , respectively. According to Figure 2, we have  $z^{-\alpha}\hat{\mathbf{C}}(z) = \mathbf{H}_p(z^{M_0})\Delta_\beta(z)\mathbf{F}_p(z^{M_0})\mathbf{C}(z)$ , with  $\Delta_\beta(z)$  defined on Figure 2. Therefore,

$$\mathbf{T}(z) = z^\alpha \mathbf{H}_p(z^{M_0})\Delta_\beta(z)\mathbf{F}_p(z^{M_0}). \quad (4)$$

Let us also represent the transmission and reception prototypes thanks to their  $M_0N$  type-I polyphase components  $K_l(z) = \sum_n f[l+nM_0N]z^{-n}$  and  $G_l(z) = \sum_n h[l+nM_0N]z^{-n}$ , respectively. Then we have

$$F_m(z) = \omega^{m(D/2)} \sum_{l=0}^{M_0N-1} z^{-l} \omega^{-ml} K_l(z^{M_0N}), \quad (5)$$

$$H_m(z) = \omega^{m(D/2)} \sum_{l=0}^{M_0N-1} z^{-l} \omega^{-ml} G_l(z^{M_0N}),$$

hence  $F_{l,m}(z) = \omega^{-ml} \omega^{m(D/2)} K_l(z)$ ,  $H_{m,l}(z) = \omega^{-ml} \omega^{m(D/2)} G_l(z)$ . The polyphase matrices  $\mathbf{F}_p(z)$  and  $\mathbf{H}_p(z)$  can then be rewritten as a product of three matrices. Thus, denoting  $\mathbf{D}_K(z) = \text{diag}[K_0(z), \dots, K_{M_0N-1}(z)]$ ,  $\mathbf{D}_G(z) = \text{diag}[G_0(z), \dots, G_{M_0N-1}(z)]$ ,  $\mathbf{D}_\omega = \text{diag}[1, \omega, \dots, \omega^{M-1}]$ , and

$$\mathbf{W}_{M \times M_0N} = \begin{pmatrix} 1 & 1 & \cdots & 1 \\ 1 & \omega & \cdots & \omega^{M_0N-1} \\ \vdots & \vdots & \ddots & \vdots \\ 1 & \omega^{M-1} & \cdots & \omega^{(M-1)(M_0N-1)} \end{pmatrix}, \quad (6)$$

we get  $\mathbf{F}_p(z) = [\mathbf{D}_\omega^{D/2} \mathbf{W}_{M \times M_0N}^* \mathbf{D}_K(z)]^T$  and  $\mathbf{H}_p(z) = \mathbf{D}_\omega^{D/2} \mathbf{W}_{M \times M_0N}^* \mathbf{D}_G(z)$ . Therefore, we obtain a transfer matrix written as

$$\mathbf{T}(z) = z^\alpha \mathbf{D}_\omega^{D/2} \mathbf{W}_{M \times M_0N}^* \mathbf{D}_G(z^{M_0}) \Delta_\beta(z) \times \mathbf{D}_K(z^{M_0}) \mathbf{W}_{M \times M_0N}^T \mathbf{D}_\omega^{D/2}. \quad (7)$$

Let us now compute  $\Delta_\beta(z)$ . The component  $[\Delta_\beta]_{l,l'}(z)$  of  $\Delta_\beta(z)$  with coordinates  $l, l'$  is exactly a delay  $z^{-(l+l'+\beta)}$  placed between an  $N$ -order expander and an  $N$ -order decimator. So, we deduce that  $[\Delta_\beta]_{l,l'}(z) = z^{-(l+l'+\beta)/N} d_{l+l'+\beta,N}$ , with  $d_{m,n} = 1$  if  $m$  is a multiple of  $n$  and 0 otherwise. And, after some computations, we finally get that for  $0 \leq k, k' \leq M-1$ ,

$$\begin{aligned} [\mathbf{T}]_{k,k'}(z) &= z^\alpha \omega^{(k+k')(D/2)} \\ &\times \sum_{l,l'=0}^{M_0N-1} z^{-(l+l'+\beta)/N} \omega^{-(kl+k'l')} G_l(z^{M_0}) K_{l'}(z^{M_0}) d_{l+l'+\beta,N}. \end{aligned} \quad (8)$$

The transfer matrix entries involve a double sum with an important number of elements equal to zero. In order to only keep the nonzero elements, we only consider the values of  $l'$  so that  $l+l'+\beta$  is a multiple of  $N$ . In this case, if we denote

$$\Lambda_\beta = \begin{cases} \{0, \dots, M_0-1\} & \text{when } \beta = 0, \\ \{1, \dots, M_0\} & \text{when } \beta > 0, \end{cases} \quad (9)$$

then for each  $l$  so that  $0 \leq l \leq M_0N-1$ , there exists a unique  $\lambda \in \Lambda_\beta$  so that  $l' = \lambda N - \beta - l$  if  $0 \leq l \leq \lambda N - \beta$  and  $l' = (\lambda + M_0)N - \beta - l$  if  $\lambda N - \beta + 1 \leq l \leq M_0N-1$ . This leads us to define the parameter  $\epsilon_l^\lambda$  and the filter  $U_l^\lambda(z)$  by

$$\epsilon_l^\lambda = \begin{cases} 0 & \text{if } 0 \leq l \leq \lambda N - \beta, \\ 1 & \text{if } \lambda N - \beta + 1 \leq l \leq M_0N - 1, \end{cases} \quad (10)$$

$$U_l^\lambda(z) = z^{-\epsilon_l^\lambda} G_l(z) K_{(\lambda + \epsilon_l^\lambda)M_0N - \beta - l}(z). \quad (11)$$

Hence, from (8), we finally get that

$$\begin{aligned} [\mathbf{T}]_{k,k'}(z) &= z^\alpha \omega^{(k+k')(D/2) + \beta k'} \\ &\times \sum_{\lambda \in \Lambda_\beta} \omega^{-k'\lambda N} z^{-\lambda} \sum_{l=0}^{M_0N-1} \omega^{-l(k-k')} U_l^\lambda(z^{M_0}). \end{aligned} \quad (12)$$

### 3. PERFECT RECONSTRUCTION THEOREMS

The previous computations were a necessary first step to get the PR conditions in the polyphase domain with respect to the FIR causal prototypes. In this section, we provide the complete derivation of these PR conditions, presented at first in [5], for oversampled BFDN/QAM systems. Then, we present a decomposition theorem that leads to a substantial simplification of the initial system of PR equations.

#### 3.1. Biorthogonality conditions

In the  $z$ -transform domain, the biorthogonality conditions simply write  $\mathbf{T}(z) = \mathbf{I}$ . In order to simplify (7), we can first note that  $\mathbf{W}_{M \times M_0 N}^* \mathbf{W}_{M \times M_0 N}^T = M_0 N \mathbf{I}$ . Therefore,  $\mathbf{W}_{M \times M_0 N}^T$  and  $\mathbf{W}_{M \times M_0 N}$  are left-invertible and right-invertible, respectively. Moreover, as  $\mathbf{D}_\omega$  is diagonal, and therefore invertible, the equation obtained by multiplication on the left by  $\mathbf{D}_\omega^{-D/2} \mathbf{W}_{M \times M_0 N}^T$  and on the right by  $\mathbf{W}_{M \times M_0 N} \mathbf{D}_\omega^{-D/2}$ , of the two members of the equality  $\mathbf{T}(z) = \mathbf{I}$ , remains equivalent to  $\mathbf{T}(z) = \mathbf{I}$ . Thus, using (7), the system achieves PR if and only if

$$\begin{aligned} \mathbf{W}_{M \times M_0 N}^T \mathbf{W}_{M \times M_0 N}^* \mathbf{D}_G(z^{M_0}) \Delta_\beta(z) \mathbf{D}_K(z^{M_0}) \mathbf{W}_{M \times M_0 N}^{*T} \mathbf{W}_{M \times M_0 N} \\ = z^{-\alpha} \mathbf{W}_{M \times M_0 N}^T \mathbf{D}_\omega^{-D} \mathbf{W}_{M \times M_0 N}. \end{aligned} \quad (13)$$

For  $0 \leq l, l' \leq M_0 N - 1$ , we have  $[\mathbf{W}_{M \times M_0 N}^T \mathbf{W}_{M \times M_0 N}^*]_{l, l'} = \sum_{k=0}^{M-1} \omega^{k(l-l')} = M d_{l-l', M}$ , and  $[\mathbf{W}_{M \times M_0 N}^T \mathbf{D}_\omega^{-D} \mathbf{W}_{M \times M_0 N}]_{l, l'} = \sum_{k=0}^{M-1} \omega^{k(l+l'-D)} = M d_{l+l'-D, M}$ . Thus, the PR conditions are given by

$$\begin{aligned} \sum_{l_1, l_2=0}^{M_0 N - 1} z^{-(l_1 + l_2 + \beta)/N} G_{l_1}(z^{M_0}) K_{l_2}(z^{M_0}) d_{l-l_1, M} d_{l'-l_2, M} d_{l_1 + l_2 + \beta, N} \\ = \frac{z^{-\alpha}}{M} d_{l+l'-D, M}, \end{aligned} \quad (14)$$

which can be rewritten as

$$\sum_{\lambda \in \Lambda_\beta} \sum_{l_1=0}^{M_0 N - 1} z^{-\lambda} U_{l_1}^\lambda(z^{M_0}) d_{l-l_1, M} d_{l'+l_1+\beta-\lambda N, M} = \frac{z^{-\alpha}}{M} d_{l+l'-D, M}. \quad (15)$$

Therefore, we obtain two types of relation, according to whether  $l + l' - D$  is a multiple of  $M$  or not.

- (i) If  $l + l' - D$  is a multiple of  $M$ , in this case,  $d_{l'+l_1+\beta-\lambda N, M}$  is equal to  $d_{l-l_1+(\lambda-\alpha)N, M}$  and to  $d_{(\lambda-\alpha)N, M}$ , which also writes  $d_{(\lambda-\alpha)N_0, M_0}$ , or  $d_{\lambda-\alpha, M_0}$ . Therefore, we finally get  $d_{l-l_1, M} d_{l'+l_1+\beta-\lambda N, M} = d_{l-l_1, M} d_{\lambda-\alpha, M_0}$ . Thus, denoting by  $\lambda_0$  the unique element of  $\Lambda_\beta$  so that  $\lambda_0 \equiv \alpha \pmod{M_0}$ , the first type of relation writes, for  $0 \leq l \leq M_0 N - 1$ ,

$$\sum_{l_1=0}^{M_0 N - 1} z^{-\lambda_0} U_{l_1}^{\lambda_0}(z^{M_0}) d_{l-l_1, M} = \frac{z^{-\alpha}}{M}. \quad (16)$$

Thus, these  $M_0 N$  equations reduce in fact to  $M$  equations given by

$$\sum_{n=0}^{N_0-1} z^{-\lambda_0} U_{nM+l}^{\lambda_0}(z) = \frac{z^{-(\alpha-\lambda_0)/M_0}}{M}, \quad 0 \leq l \leq M-1. \quad (17)$$

- (ii) If  $l + l' - D$  is not a multiple of  $M$ , the same argumentation leads to

$$\sum_{n=0}^{N_0-1} z^{-\lambda} U_{nM+l}^\lambda(z) = 0, \quad (18)$$

for  $\lambda - \alpha$  nonmultiple of  $M_0$  (i.e.,  $\lambda \neq \lambda_0$ ) and for  $0 \leq l \leq M-1$ .

From (11), (17), and (18), we can deduce that the reconstruction is perfect with a delay  $\alpha$  if and only if for  $0 \leq l \leq M-1$  and for  $\lambda \in \Lambda_\beta$ ,

$$\begin{aligned} \sum_{n=0}^{n_{l,\lambda}} G_{nM+l}(z) K_{\lambda N - \beta - (nM+l)}(z) \\ + z^{-1} \sum_{n=n_{l,\lambda}+1}^{N_0-1} G_{nM+l}(z) K_{(\lambda+M_0)N - \beta - (nM+l)}(z) \\ = \frac{z^{-(\alpha-\lambda)/M_0}}{M} d_{\lambda-\alpha, M_0}, \end{aligned} \quad (19)$$

with  $n_{l,\lambda} = \lfloor (\lambda N - \beta - l)/M \rfloor$ , which can still be rewritten under a different form defining the integer parameters  $s_0$  and  $d_0$  by

$$D = s_0 M_0 N + d_0, \quad 0 \leq d_0 \leq M_0 N - 1. \quad (20)$$

The  $s_0$  and  $d_0$  parameters are related to the  $\alpha$  and  $\beta$ , defined by (2), by

$$s_0 = \frac{\alpha - \lambda_0}{M_0}, \quad d_0 = \lambda_0 N - \beta. \quad (21)$$

Therefore, we deduce the following theorem.

**Theorem 1.** *A signal transmitted by a BFDN/QAM system (see Figure 2) can be perfectly recovered at the reception side, in absence of perturbation along the transmission channel if and only if for  $0 \leq l \leq M-1$  and  $\lambda \in \Lambda_\beta$ ,*

$$\begin{aligned} \sum_{n=0}^{n_{l,\lambda}} G_{nM+l}(z) K_{(\lambda-\lambda_0)N + d_0 - (nM+l)}(z) \\ + z^{-1} \sum_{n=n_{l,\lambda}+1}^{N_0-1} G_{nM+l}(z) K_{(\lambda-\lambda_0+M_0)N + d_0 - (nM+l)}(z) \\ = \frac{z^{-s_0}}{M} \delta_{\lambda, \lambda_0}, \end{aligned} \quad (22)$$

with

$$n_{l,\lambda} = \left\lfloor \frac{(\lambda - \lambda_0)N + d_0 - l}{M} \right\rfloor \quad (23)$$

and  $\Lambda_\beta = \{0, \dots, M_0 - 1\}$  if  $\beta = 0$ ,  $\Lambda_\beta = \{1, \dots, M_0\}$  else.



Orthogonality is a restriction of biorthogonality and corresponds to the case where  $D = L_f - 1$  and  $h[k] = f^*[L_f - 1 - k]$ , which also writes  $H(z) = z^{-(L_f-1)}\tilde{F}(z)$ . Using this notation, a rewriting of Theorem 1, not taking into account the reconstruction delay, allows the recovering of orthogonality conditions identical, with the exception of a normalization factor, to the ones obtained in [3] for oversampled OFDM and in [20] for tight Weyl-Heisenberg frames in  $l_2(\mathbb{Z})$ .

### 3.2. Decomposition theorem in the case

$$\beta = 1 \quad (D = \alpha N - 1)$$

Theorem 1 leads to a system of  $M_0M$  linked polynomial equations. When  $\beta = 1$ , we now show that it is possible to considerably reduce the complexity of this system by splitting it into  $\Delta$  independent systems of  $M_0^2$  linked polynomial equations, with  $\Delta$  the gcd of  $M$  and  $N$ .

Let us first notice that if  $\Delta = \text{gcd}(M, N)$ , then  $MN = \Delta \text{lcm}(M, N) = \Delta M_0 N$ , which shows that  $M = M_0 \Delta$  and  $N = N_0 \Delta$ .

Let us now define  $A_l^{(p)}(z)$  and  $B_l^{(p)}(z)$ ,  $0 \leq l \leq M_0 N_0 - 1$ ,  $0 \leq p \leq \Delta - 1$ , by

$$A_l^{(p)}(z) = \sqrt{M} G_{l\Delta+p}(z), \quad B_l^{(p)}(z) = \sqrt{M} K_{l\Delta+p}(z). \quad (24)$$

$A_l^{(p)}(z)$  and  $B_l^{(p)}(z)$  are linked to the prototypes  $H(z)$  and  $F(z)$  by

$$H(z) = \frac{1}{\sqrt{M}} \sum_{l=0}^{M_0 N_0 - 1} \sum_{p=0}^{\Delta-1} z^{-(l\Delta+p)} A_l^{(p)}(z^{M_0 N}), \quad (25)$$

$$F(z) = \frac{1}{\sqrt{M}} \sum_{l=0}^{M_0 N_0 - 1} \sum_{p=0}^{\Delta-1} z^{-(l\Delta+p)} B_l^{(p)}(z^{M_0 N}). \quad (26)$$

Moreover, for  $l = k\Delta + p$ ,  $0 \leq p \leq \Delta - 1$ , and  $0 \leq k \leq M_0 - 1$ ,

$$G_{nM+l}(z) = G_{nM_0\Delta+k\Delta+p}(z) = G_{(nM_0+k)\Delta+p}(z) = \frac{1}{\sqrt{M}} A_{nM_0+k}^{(p)}(z),$$

$$\begin{aligned} K_{\lambda N - 1 - (nM+l)}(z) &= K_{\lambda N_0 \Delta - 1 - (nM_0 \Delta + k\Delta + p)}(z) \\ &= K_{(\lambda N_0 - 1 - (nM_0 + k))\Delta + \Delta - 1 - p}(z) \\ &= \frac{1}{\sqrt{M}} B_{\lambda N_0 - 1 - (nM_0 + k)}^{(\Delta-1-p)}(z), \end{aligned}$$

$$\begin{aligned} K_{M_0 N + \lambda N - 1 - (nM+l)}(z) &= K_{M_0 N_0 \Delta + \lambda N_0 \Delta - 1 - (nM_0 \Delta + k\Delta + p)}(z) \\ &= K_{(M_0 N_0 + \lambda N_0 - 1 - (nM_0 + k))\Delta + \Delta - 1 - p}(z) \\ &= \frac{1}{\sqrt{M}} B_{M_0 N_0 + \lambda N_0 - 1 - (nM_0 + k)}^{(\Delta-1-p)}(z). \end{aligned} \quad (27)$$

Let us now set  $n_{k,\lambda}^{(p)} = n_{k\Delta+p,\lambda}$ . Using the fact that  $\beta = 1$ , it appears that

$$n_{k,\lambda}^{(p)} = \left\lfloor \frac{\lambda N_0 - 1 - k}{M_0} \right\rfloor. \quad (28)$$

Thus,  $n_{k,\lambda}^{(p)}$  does not depend upon  $p$  and the equalities (27) and (28) associated to Theorem 1 lead to the following decomposition theorem.

**Theorem 2.** *An oversampled complex modulated transmultiplexer with  $\beta = 1$  achieves PR if and only if for  $0 \leq p \leq \Delta - 1$ ,  $0 \leq k \leq M_0 - 1$ , and  $1 \leq \lambda \leq M_0$ ,*

$$\begin{aligned} &\sum_{n=0}^{n_{k,\lambda}^{(0)}} A_{nM_0+k}^{(p)}(z) B_{\lambda N_0 - 1 - (nM_0+k)}^{(\Delta-1-p)}(z) \\ &\quad + z^{-1} \sum_{n=n_{k,\lambda}^{(0)}+1}^{N_0-1} A_{nM_0+k}^{(p)}(z) B_{N_0 M_0 + \lambda N_0 - 1 - (nM_0+k)}^{(\Delta-1-p)}(z) \\ &= z^{-s_0} \delta_{\lambda, \lambda_0}, \end{aligned} \quad (29)$$

with  $n_{k,\lambda}^{(0)} = \lfloor (\lambda N_0 - 1 - k)/M_0 \rfloor$ .

This theorem may have very strong practical implications. Suppose, for instance, that the initial problem was to design an oversampled OFDM system with  $M = 1024$  carriers and an oversampling ratio  $r = 3/2$ . A direct approach leads to a problem with 2048 equations while thanks to the decomposition theorem, we can choose to first solve a subsystem of  $M_0^2 = 4$  equations and then we have to find a method providing an appropriate global solution for the 512 independent subsystems. Let us now explain how these two remaining problems can be solved.

## 4. PARAMETRIZATION IN THE ORTHOGONAL CASE

The parametrization of the polyphase matrices related to oversampled DFT transmultiplexers can be formulated as the factorization of the Gabor frame operator [25]. But to get the explicit expression of each prototype's coefficient as a function of the parameters, we need to go a step further. On the other hand, using the parametrization proposed in [20] for oversampled DFT filter banks does not guarantee the covering of the whole set of solutions. In this section, we focus on the important case of linear-phase real-valued orthogonal prototype filters. We also suppose that the prototype filter length is  $L = mM_0N$ , that is, each polyphase component has an identical degree  $(m - 1)$ . Our approach leads to an angular parametrization of the whole set of orthogonal solutions. This parametrization is illustrated by means of a simple example.

### 4.1. Exact resolution method

Owing to our assumptions, we now have the following equalities:  $L = L_f = L_h = D + 1 = mM_0N$ ,  $H(z) = z^{-(L-1)}F(z^{-1}) = F(z)$ . That means that the parameters defined in (20)-(21) are such that  $\beta = 1$ ,  $s_0 = m - 1$ ,  $d_0 = M_0N - 1$ ,  $\lambda_0 = M_0$ . With this particular set of values, the PR conditions are now given, for  $0 \leq l \leq M - 1$  and  $1 \leq \lambda \leq M_0$ , by

$$\begin{aligned} &\sum_{n=0}^{n'_{l,\lambda}} G_{nM+l}(z) \tilde{G}_{nM+l+(M_0-\lambda)N}(z) \\ &\quad + z^{-1} \sum_{n=n'_{l,\lambda}+1}^{N_0-1} G_{nM+l}(z) \tilde{G}_{nM+l-\lambda N_0}(z) = \frac{\delta_{\lambda, M_0}}{M}, \end{aligned} \quad (30)$$

with  $n'_{i,\lambda} = \lfloor (\lambda N - 1 - l)/M \rfloor$  and  $\tilde{G}_i(z) = G(1/z)$ . In this particular case, the decomposition theorem leads to a set of  $\Delta$  independent subsystems of  $M_0^2$  equations that for  $0 \leq p \leq \Delta - 1$ ,  $0 \leq k \leq M_0 - 1$ , and  $1 \leq \lambda \leq M_0$  are given by

$$\begin{aligned} & \sum_{n=0}^{n_{k,\lambda}^{(0)}} A_{nM_0+k}^{(p)}(z) \tilde{A}_{nM_0+k+(M_0-\lambda)N_0}^{(p)}(z) \\ & + z^{-1} \sum_{n=n_{k,\lambda+1}^{(0)}}^{N_0-1} A_{nM_0+k}^{(p)}(z) \tilde{A}_{nM_0+k-\lambda N_0}^{(p)}(z) \\ & = \delta_{\lambda, M_0}. \end{aligned} \quad (31)$$

With  $F(z)$  being linear-phase, this system can be further reduced to  $\Delta/2$  subsystems.

The approach proposed in [20] to solve a similar set of algebraic equations consists in connecting the orthogonal prototypes to some general paraunitary matrices. This approach, as in [2, 3], amounts to solve nonsquare systems of algebraic equations using general factorization procedures [24] and optimization without explicitly taking into account the specific features of these systems. Here, we take advantage of the decomposition theorem to derive the whole set of potential solutions on a parametrical form depending on each triplet  $(M_0, N_0, m)$ .

As the  $\Delta$  subsystems defined by (31) are independent, but formally equivalent, we only need to describe the resolution of one of them. Thus, for notational convenience, we now omit the superscript  $(p)$  in (31) and we denote the resulting subsystem by  $\mathcal{S}_{M_0, N_0, m}$ . These subsystems can be exactly solved using the notion of *admissible systems* and two types of operations named *splitting* and *rotation*, introduced at first in [21]. So, let us consider the  $\mathcal{S}_{2,3,1}$  subsystem. In this case, for a symmetrical prototype, we have  $\Delta/2$  independent sets of  $M_0^2 = 4$  equations so that

$$\begin{aligned} A_0(z) \tilde{A}_3(z) + A_2(z) \tilde{A}_5(z) + z^{-1} A_4(z) \tilde{A}_1(z) &= 0, \\ A_1(z) \tilde{A}_4(z) + z^{-1} A_3(z) \tilde{A}_0(z) + z^{-1} A_5(z) \tilde{A}_2(z) &= 0, \\ A_0(z) \tilde{A}_0(z) + A_2(z) \tilde{A}_2(z) + A_4(z) \tilde{A}_4(z) &= 1, \\ A_1(z) \tilde{A}_1(z) + A_3(z) \tilde{A}_3(z) + A_5(z) \tilde{A}_5(z) &= 1. \end{aligned} \quad (32)$$

For each  $A_i(z)$ ,  $i = 0, \dots, M_0 N_0 - 1$ , we denote

$$A_i(z) = \sum_{k=0}^{m-1} a_{i,k} z^{-k}. \quad (33)$$

For our example,  $m = 1$ , and to simplify the notation, we set  $A_i(z) = a_i$ , then (32) are equivalent to

$$a_0^2 + a_2^2 + a_4^2 = 1, \quad a_1^2 + a_3^2 + a_5^2 = 1, \quad (34)$$

$$a_0 a_3 + a_2 a_5 = 0, \quad a_1 a_4 = 0. \quad (35)$$

### Admissible systems

In system (34)-(35), we can easily distinguish two types of equations: (34) that are called *square equations* and (35) named *orthogonal equations*. We can also notice the existence of partitions of the variables associated to these two

types of equations. So, we can say that  $\mathcal{P}_S = \{\{a_0, a_2, a_4\}, \{a_1, a_3, a_5\}\}$  is the *partition of the squares* and  $\mathcal{P}_O = \{\{a_0, a_3\}, \{a_1, a_4\}, \{a_2, a_5\}\}$  is the partition associated to the orthogonal equations. We say that a system of algebraic equations composed of orthogonal and square equations, and for which there exist a partition  $\mathcal{P}_S$  and a partition  $\mathcal{P}_O$ , is *admissible*. An admissible system without orthogonal equation is called *trivial*. In this case, the system is composed of  $n$  independent systems, where  $n$  is the cardinal of  $\mathcal{P}_S$ . Each square equation then admits some solutions that can be represented thanks to  $k - 1$  independent angular parameters if  $k$  is the number of variables of the equation. If  $k = 1$ , the equation is of the form  $x^2 = 1$  and its solutions are  $x = \pm 1$ . If  $k > 1$ , the solution is of the form

$$x_1 = \prod_{i=1}^{k-1} \cos \theta_i, \quad x_n = \sin \theta_{n-1} \prod_{i=n}^{k-1} \cos \theta_i, \quad n = 2, \dots, k. \quad (36)$$

The initial systems, deduced from (31), are admissible. The resolution method consists of replacing an initial system by a set of trivial equivalent systems thanks to a sequence of two types of transformations:

(1) the *splitting*, which replaces an admissible system by an equivalent set of systems. Only the nonredundant resulting systems are kept. For instance, it can easily be seen that the system (34)-(35) can be split thanks to (35), setting either  $a_1 = 0$  or  $a_4 = 0$ ,

(2) the *rotation*, which operates a substitution of variables, depending upon an angular parameter, over an admissible system replacing it by an equivalent system.

The rotation is used for systems that cannot be split. Let  $\mathcal{S}$  be an admissible system that cannot be split. Suppose that there exist two distinct subsets  $O_1$  and  $O_2$  of its partition  $\mathcal{P}_O$  and a one-to-one correspondence  $\phi : O_1 \rightarrow O_2$  satisfying the following properties:

- (1) for all  $x \in O_1$ ,  $x$  and  $\phi(x)$  belong to the same subset of the partition  $\mathcal{P}_S$ ;
- (2) for all orthogonal equations containing the monomial  $xy$  with  $x, y \in O_1$ , then the same equation contains the monomials  $\phi(x)\phi(y)$  elements of  $O_2$ .

We then say that the system is *regular*. The subsets  $O_1$  and  $O_2$  therefore have the same number of elements, greater or equal to 2. We denote by  $\{x_1, x_2, \dots, x_k\}$  the elements of  $O_1$  and  $\{y_1, y_2, \dots, y_k\}$  the elements of  $O_2$  with  $y_i = \phi(x_i)$ ,  $i = 1, \dots, k$ . Let  $\theta$  be an angular parameter. The rotation consists of replacing  $x_i$  and  $y_i$  by

$$\begin{aligned} \begin{bmatrix} x_1 \\ y_1 \end{bmatrix} &= \begin{bmatrix} r_1 \cos \theta \\ r_1 \sin \theta \end{bmatrix}, \\ \begin{bmatrix} x_i \\ y_i \end{bmatrix} &= \begin{bmatrix} \cos \theta & -\sin \theta \\ \sin \theta & \cos \theta \end{bmatrix} \begin{bmatrix} r_i \\ s_i \end{bmatrix}, \end{aligned} \quad (37)$$

where  $r_1, r_i, s_i$ ,  $i = 2, \dots, k$  are the new variables. We denote the resulting system by  $\mathcal{R}$ . The sum  $x_1^2 + y_1^2$  which occurs in one of the square equations, since  $x_1$  and  $y_1$  belong to the same subset of the square partition, is replaced by  $r_1^2$  and

similarly, for  $i = 2, \dots, k$ , we have

$$x_i^2 + y_i^2 = r_i^2 + s_i^2. \quad (38)$$

In the orthogonal equations, we have the groups  $x_1x_i + y_1y_i$ ,  $i = 2, \dots, k$ , or  $x_ix_j + y_iy_j$ ,  $2 \leq i, j \leq k$ ,  $i \neq j$ . Then, we get

$$x_1x_i + y_1y_i = r_1r_i, \quad (39)$$

$$x_ix_j + y_iy_j = r_jr_i + s_js_i. \quad (40)$$

The obtained system is admissible. The  $2k$  variables  $x_1, \dots, x_k, y_1, \dots, y_k$  are replaced by the  $2k - 1$  variables  $r_1, \dots, r_k, s_2, \dots, s_k$  and the partition  $\mathcal{P}_O$  is replaced by the partition obtained when replacing the subset  $O_1$  by the subset  $\{r_1, \dots, r_k\}$  and  $O_2$  by  $\{s_2, \dots, s_k\}$ .

If one or several orthogonal equations of  $\mathcal{S}$  are identical to the left-hand side of (39), we see that the obtained system  $\mathcal{R}$  can be split.

*Remark 1.* There is no guarantee that the system  $\mathcal{R}$  is regular if it cannot be split, nor that the systems obtained after a splitting of  $\mathcal{R}$  are regular.

As for  $\mathcal{S}_{2,3,1}$ , the two subsystems derived from (34)-(35) obtained after the first splitting operation are both regular. Considering, for example, the first one, obtained with  $a_1 = 0$ , we see that we have the one-to-one correspondence  $a_2 = \phi(a_0)$  and  $a_5 = \phi(a_3)$ . Thus, we make the following variable substitution:

$$\begin{aligned} \begin{bmatrix} a_0 \\ a_2 \end{bmatrix} &= \begin{bmatrix} r_0 \cos \theta_0 \\ r_0 \sin \theta_0 \end{bmatrix}, \\ \begin{bmatrix} a_3 \\ a_5 \end{bmatrix} &= \begin{bmatrix} \cos \theta_0 & -\sin \theta_0 \\ \sin \theta_0 & \cos \theta_0 \end{bmatrix} \begin{bmatrix} r_1 \\ s_1 \end{bmatrix}, \end{aligned} \quad (41)$$

and we get the equivalent system composed by the three equations  $r_1^2 + s_1^2 = 1$ ,  $r_0^2 + a_4^2 = 1$ , and  $r_0r_1 = 0$ . We observe that we get another system that can be split.

It can easily be seen that (34)-(35), and more generally, all subsystems derived from (30) are admissible. So for any subsystem, the resolution method is to operate splitting and rotation transformations until trivial systems are produced and all of their solutions are derived. Even if, until now, the validity of our method is not proved for any system, we can exhibit many examples showing that it is successful for various sets of values of  $M_0$ ,  $N_0$ , and  $m$ . For instance, at the end, for the  $\mathcal{S}_{2,3,1}$  subsystem, it can be easily checked that we get the three following parametrical solutions:

$$\begin{cases} a_0 = a_1 = a_2 = 0, \\ a_3 = \cos \theta_0 \cos \theta_1 - \sin \theta_0 \sin \theta_1 = \cos(\theta_0 + \theta_1), \\ a_4 = \pm 1, \\ a_5 = \sin \theta_0 \cos \theta_1 + \cos \theta_0 \sin \theta_1 = \sin(\theta_0 + \theta_1), \end{cases} \quad (42)$$

$$\begin{cases} a_0 = \cos \theta_0 \cos \theta_1, \\ a_1 = 0, \\ a_2 = \sin \theta_0 \cos \theta_1, \\ a_3 = -\sin \theta_0, \\ a_4 = \sin \theta_1, \\ a_5 = \cos \theta_0, \end{cases} \quad \begin{cases} a_0 = \cos \theta_0, \\ a_1 = \cos \theta_1, \\ a_2 = \sin \theta_0, \\ a_3 = -\sin \theta_0 \sin \theta_1, \\ a_4 = 0, \\ a_5 = \cos \theta_0 \sin \theta_1. \end{cases} \quad (43)$$

The  $\mathcal{S}_{2,3,1}$  example is very simple since there are only 3 solutions. But the calculus can rapidly become very heavy. For example,  $\mathcal{S}_{4,5,2}$  leads to 13502 solutions. Therefore, not all of these exact parametrical solutions can be kept for the design step. The proposed heuristic is only to retain the solutions with the best potential of optimization taking into account the dimension of the solution as computed in the appendix. Indeed, we have noticed that subsystems with solutions of maximal dimensions provide the best design results after optimization. In the case of  $\mathcal{S}_{2,3,1}$ , we immediately see that solutions (43) are of maximal dimension 2. Setting  $\cos(\theta_1) = 0$ , it can also be noted that (42) is a particular case of the first solution given in (43). For high-order subsystems, even if in general, the solutions of maximum dimension does not contain the whole set of solutions, this selection by the dimension becomes of paramount importance. As a matter of example, for the  $\mathcal{S}_{4,5,2}$  system starting from the 13502 solutions, we could only find 16 having the best features, that is, a dimension equal to 12 in this case.

#### 4.2. Parametrization of the orthogonal symmetrical prototype

The solutions of each subsystem, that is, the  $M_0N_0$  filters  $A_i(z)$ , are given for a particular value of  $p$ , therefore for a given subset of polyphase components. To recover the coefficients of the impulse response  $f[k]$ , we have to take into account the way the polyphase components have been regularly interleaved by the polyphase decomposition, see Section 2.3 and (24) and (25), in the particular case of a symmetrical prototype. So, we now have to come back to the initial and more general notation. Thus, we have to consider  $\Delta$  independent subsystems, involving the filters  $A_i^{(p)}(z)$ ,  $0 \leq p \leq \Delta - 1$ , or  $\Delta/2$  in the case of symmetrical prototype. For some values of  $M_0$ ,  $N_0$ ,  $m$ , and  $\Delta$ , let us denote by  $|\theta|$  the number of angular parameters corresponding to the parametrization of each of the  $\Delta/2$  subsystems  $\mathcal{S}_{M_0, N_0, m}$ . Each of these systems could be parameterized with a different solution, thus leading to different values of  $|\theta|$ . For simplicity, we assume that the same exact parametrical solution is used for each subsystem. So, for any design problem, the prototype filter  $f[k]$  is expressed as a function of the angular parameters  $\theta_i^{(p)}$ , with  $i = 0, \dots, |\theta|$ ,  $p = 0, \dots, \Delta/2 - 1$ . So, we have  $(\Delta/2)|\theta|$  parameters to optimize. Naturally, if we want to be almost sure to get the ‘‘best’’ design result, we have to test all of the parametrical sets of higher dimensions. For instance, if the design parameters are such that  $m = 2$  and  $r = 5/4$  (i.e., correspond to the  $\mathcal{S}_{4,5,2}$  subsystem), the following design step will be carried out with the 16 ‘‘best’’ solutions.

### 5. DESIGN METHOD AND EXAMPLES

The design problem consists of finding the coefficients of the prototype filter that satisfy some optimization criterion. Here we consider two different criteria: the out-of-band energy minimization also used for instance in [10, 12] and the time-frequency localization maximization as in [11–15]. The first one leads to the minimization of the normalized out-of-band



energy expressed as

$$E = \frac{J(f_c)}{J(0)}, \quad \text{with } J(x) = \int_x^{1/2} |F(e^{j2\pi\nu})|^2 d\nu, \quad (44)$$

with  $f_c$  the cutoff frequency and considering a normalized frequency, that is, a sampling frequency equal to 1. With this definition, the out-of-band energy is always in the interval  $[0, 1]$ . In our designs, we set  $f_c = 1/M$ .

Our second design criterion is the time-frequency localization for discrete-time signals. It is given, as in [22], by

$$\xi = \frac{1}{\sqrt{4m_2M_2}}, \quad (45)$$

where  $m_2$  and  $M_2$  correspond to second-order moments in time and frequency as, originally, defined in [26]. With this definition, it can be checked that  $\xi = 1$  corresponds to the optimum.

For a multicarrier system with a high number of carriers, a direct optimization of the  $f[k]$  coefficients is not really feasible. An alternative to avoid a huge optimization problem may be to use an orthogonalization method based on the Zak transform. Indeed, its implementation avoids any optimization procedure and only requires an initial filter, and in discrete-time it can also take advantage of a fast computation based on FFTs [14]. However, until now the design examples presented are limited in size and in spectral efficiency, for example, in [8] the number of carriers is equal to 32 and the oversampling ratio is 3/2. In [19], it has been shown that when applied in continuous-time, an orthogonalization procedure such as this can lead to orthogonal functions close to the desired one. But that does not guarantee that after truncation and discretization the FIR prototype will be close to optimality, in particular if we want to get relatively short-length prototypes. For example, for OFDM/OQAM, in [12] the authors prefer to consider the out-of-band minimization of continuous-time pulse shapes with finite duration. This approach at least avoids the loss due to the truncation step. Besides, in [15], it is also shown that to get short nearly optimal prototypes for the time-frequency localization criterion, a direct design is more appropriate.

Therefore, in the following, we use the parametrical representation proposed in the previous section. Then, the expressions (44)-(45) are optimized with respect to the angular parameters  $\theta_i^{(p)}$ . Thus, the PR conditions are structurally guaranteed but the number of parameters to optimize still remains very high. For instance, if  $M = 1024$  and the oversampling ratio is equal to 3/2,  $\Delta = 512$  and we have  $256|\theta|$  parameters to optimize, with  $|\theta|$  that, for instance if  $m = 4$ , is around 10.

This is why, as in [22], we again propose to use the compact representation method. Indeed, it can be checked for both criteria, so that, as in the critically decimated case,  $\theta_i^{(p)}$  is generally a smooth function of  $p$  for fixed  $i$ . So, we assume that, at the optimum, each angular parameter leads to a smooth curve that can be easily fitted by a polynomial. Thus,

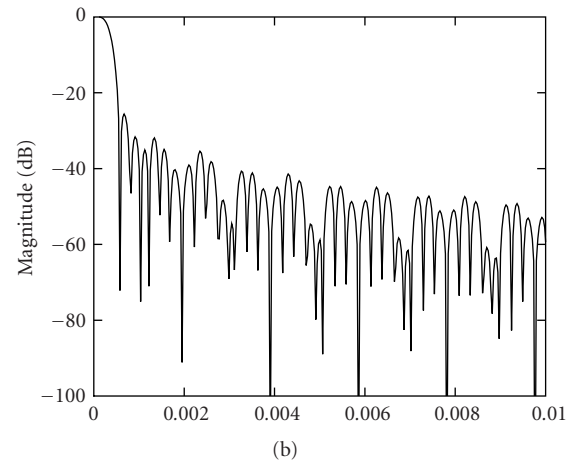
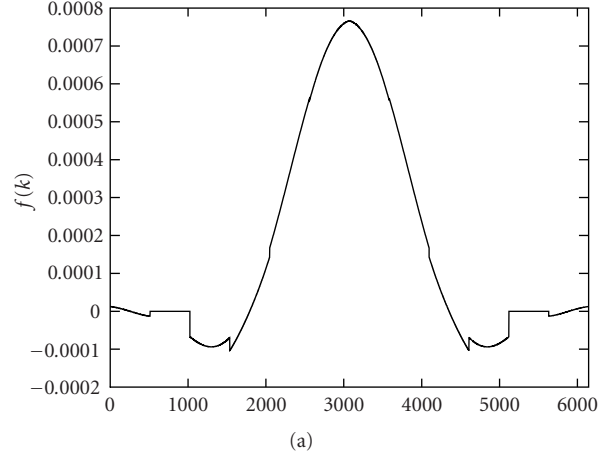


FIGURE 3: OFDM/QAM prototype filter minimizing the out-of-band energy; (a) filter coefficients and (b) frequency response, with  $M_0 = 2$ ,  $N_0 = 3$ ,  $m = 2$ ,  $M = 1024$ ,  $L = 6144$ ,  $E = 4.877638 \times 10^{-3}$ .

setting to  $K - 1$  the degree of this polynomial, we have

$$\theta_i^{(p)} = \sum_{k=0}^{K-1} x_{i,k} \left( \frac{2p+1}{2M} \right)^k, \quad i = 0, \dots, |\theta| - 1. \quad (46)$$

We then have  $K|\theta|$  parameters  $x_{i,k}$  to optimize instead of  $(\Delta/2)|\theta|$  angular parameters, if we only take advantage of the reduced system (30), and of  $mN_0M/2$  prototype coefficients in a direct approach. As in the case of critically decimated filter banks [22], it appears that a small value of  $K$  is sufficient to provide an excellent approximation. Indeed, for small values of  $M$ , it can be checked that an optimization with respect to  $x$  can provide results very close to the ones obtained when optimizing with respect to the  $\theta$ 's. This approximation can naturally lead to drastic reduction in computational complexity. For example, for all of the following design examples, we set  $K = 5$  which provides a reduction of the number of parameters  $\Delta/2K$  equal to 25.6 or 51.2.

In Figures 3, 4, 5, 6, 7, and 8, we present a set of results that have been obtained for both criteria with  $M = 1024$  and

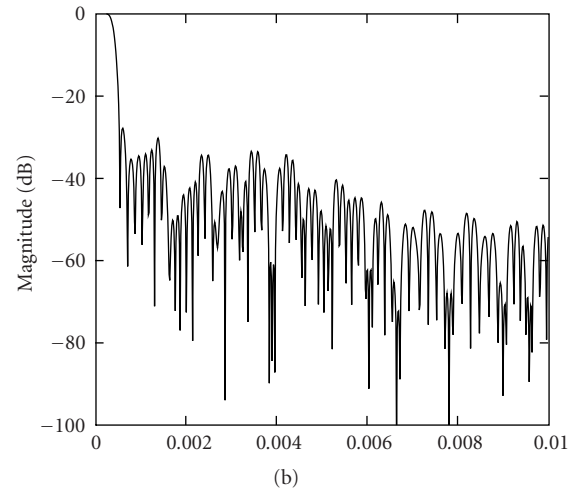
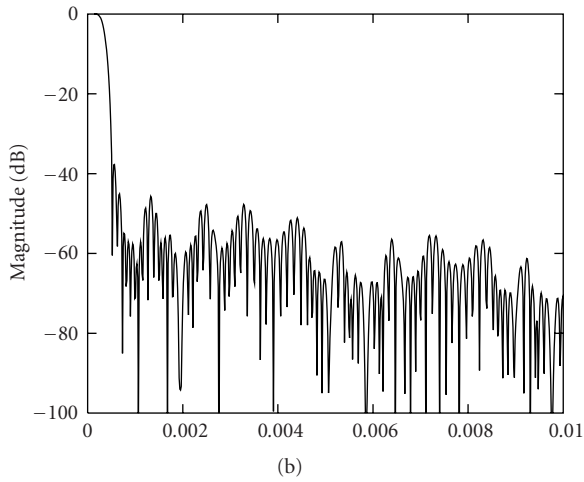
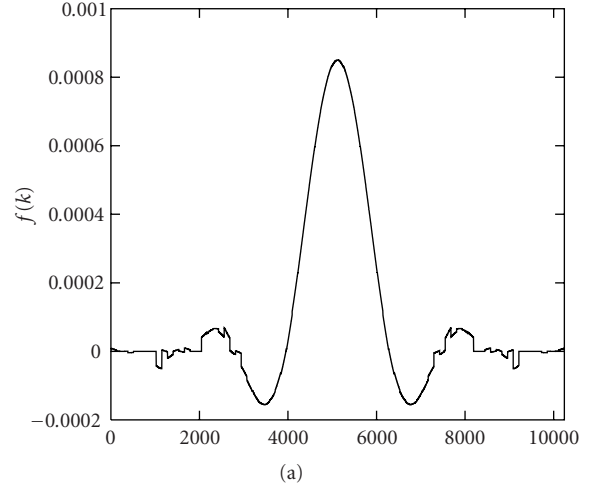
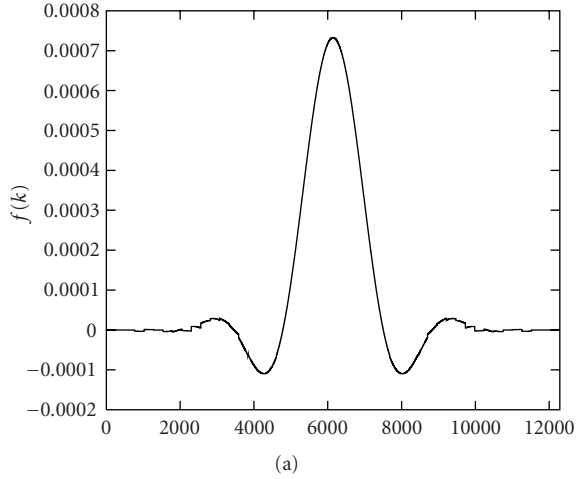


FIGURE 4: OFDM/QAM prototype filter minimizing the out-of-band energy; (a) filter coefficients and (b) frequency response, with  $M_0 = 2$ ,  $N_0 = 3$ ,  $m = 4$ ,  $M = 1024$ ,  $L = 12288$ ,  $E = 1.255076 \times 10^{-4}$ .

FIGURE 5: OFDM/QAM prototype filter minimizing the out-of-band energy; (a) filter coefficient and (b) frequency response, with  $M_0 = 4$ ,  $N_0 = 5$ ,  $m = 2$ ,  $M = 1024$ ,  $L = 10240$ ,  $E = 3.4091841 \times 10^{-3}$ .

two different oversampling ratios  $r = 3/2$  and  $r = 5/4$ . For each display, the time response is given at the left and the frequency response at the right assuming a normalized frequency, that is, a sampling frequency equal to 1. The solutions provided for  $r = 5/4$  are most interesting from a practical point of view because they correspond to a higher spectral efficiency. All of these solutions outperform, for both criteria, the one resulting from the use of a rectangular window. Indeed, their attenuation is significantly greater than the 13 dB of the  $\sin(x)/x$  function and their time-frequency localization is also significantly much higher than the  $\xi = 0.038$  provided by the rectangular window. We also naturally recover typical features related to the two different criteria: for similar values of  $m$ , the out-of-band energy leads to a narrower central lobe and to a higher attenuation of the first attenuated lobe. On the contrary time-frequency localization yields a larger central lobe but its attenuation becomes higher for increasing frequencies. In fact, perhaps, the most

interesting features are related to the difference of behavior with the two different criteria when  $m$  increases for fixed  $r$ . As it is well known in the area of filter and filter bank design, with the energy criterion the performance increases with the length of the filter: this characteristic again appears in Figures 3 and 4, increasing  $m$  from 2 to 4. In Figure 3, it appears that our result is similar to the one provided by the general parametrization method used in [2, 3]. But, differently from [2, 3], with our method we get it for 1024 carriers instead of 32. Note also that in [8], when using the Zak transform for a BFDQ/QAM system, the proposed solution is, as in [2, 3], also limited to  $M = 32$  for  $r = 3/2$ . With the time-frequency localization criterion, there is no significant difference between the results obtained for  $m = 2$ , see Figure 6 where  $\xi = 0.908548$  and  $m = 4$ , see Figure 7 where  $\xi = 0.9151744$ . Indeed, the displays show different behavior at high levels of attenuation that, therefore, do not have a strong impact on this criterion. Naturally, if as in Figure 8 we

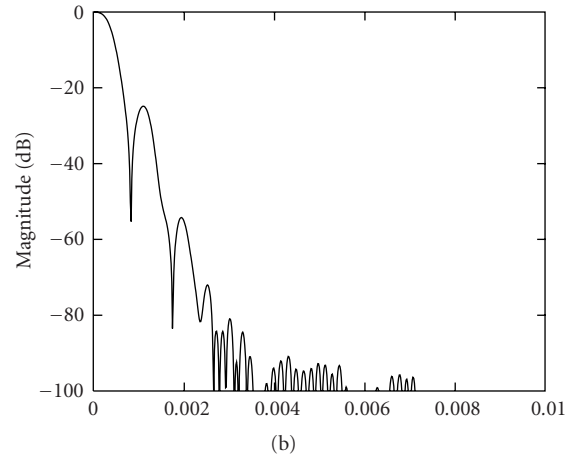
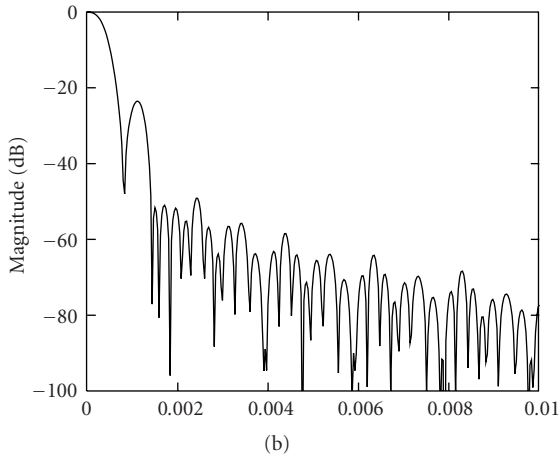
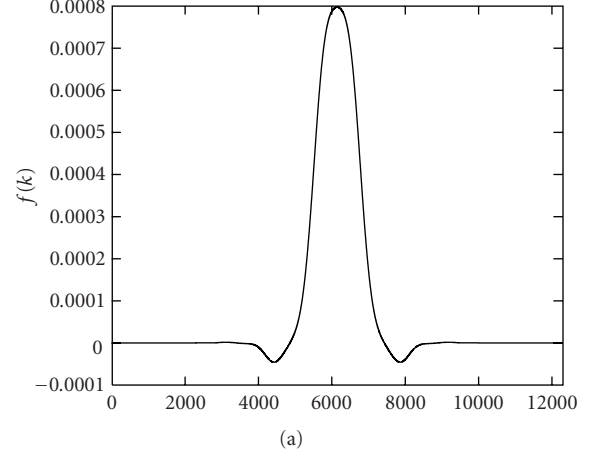
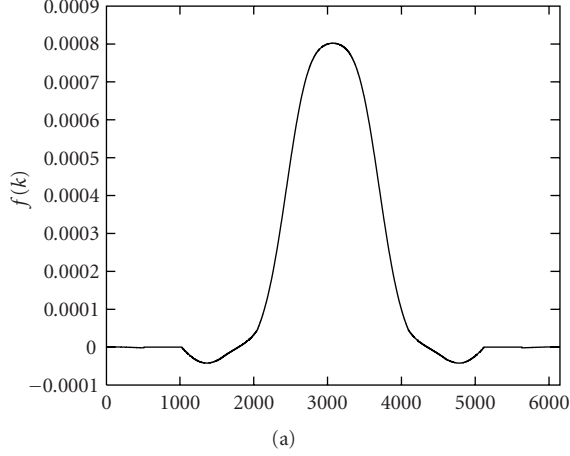


FIGURE 6: OFDM/QAM prototype filter maximizing the time-frequency localization; (a) filter coefficient and (b) frequency response, with  $M_0 = 2$ ,  $N_0 = 3$ ,  $m = 2$ ,  $M = 1024$ ,  $L = 6144$ ,  $\xi = 0.908548$ .

FIGURE 7: OFDM/QAM prototype filter maximizing the time-frequency localization; (a) filter coefficient and (b) frequency response, with  $M_0 = 2$ ,  $N_0 = 3$ ,  $m = 4$ ,  $M = 1024$ ,  $L = 12288$ ,  $\xi = 0.9157114$ .

try to get closer to critical sampling, with  $r = 5/4$ , it can be seen that the time-frequency localization decreases nevertheless staying, with  $\xi = 0.8034350$ , at an acceptable level. The fact that for the time-frequency localization criterion, relatively short prototypes (small  $m$ ) yield good results has to be emphasized. A similar behavior was already noted in the OFDM/OQAM context [15].

## 6. SIMULATION RESULTS

We now consider the transmission of the baseband signal  $s[k]$  through a Rayleigh flat fading channel. Thus,  $r[k]$  the received signal may be written as

$$r[k] = a[k]s[k] + b[k], \quad (47)$$

with  $a[k]$  a channel attenuation factor leading to a U-Doppler spectrum [27], and  $b[k]$  a complex-valued additive white Gaussian noise (AWGN) with zero mean. We denote by  $f_d$  the maximum normalized Doppler frequency.

Assuming that the channel fades sufficiently slowly ( $Mf_d \ll 1$ ), it can be shown that the demodulated symbols  $\hat{c}_{m,n}$  can be approximated thanks to

$$\hat{c}_{m,n} \approx a_n c_{m,n} + b_{m,n}, \quad (48)$$

with  $b_{m,n}$  an AWGN, with same mean and variance as  $b[k]$ , and

$$a_n = \sum_k a[k] f[k - nN] h^*[k - nN]. \quad (49)$$

Then, we can estimate the received symbols thanks to

$$\tilde{c}_{m,n} = \hat{c}_{m,n} \frac{a_n^*}{|a_n|^2 + \sigma_b^2 / \sigma_c^2}, \quad (50)$$

where  $\sigma_b^2$  and  $\sigma_c^2$  are the variance of the noise ( $b[k]$  or  $b_{m,n}$ ) and the variance of the input symbols  $c_{m,n}$ , respectively.

Signal and noise are normalized in order to get a 20 dB signal-to-noise ratio (SNR) over the channel. The attenuation factor  $a[k]$  has been generated using the rayleighchan

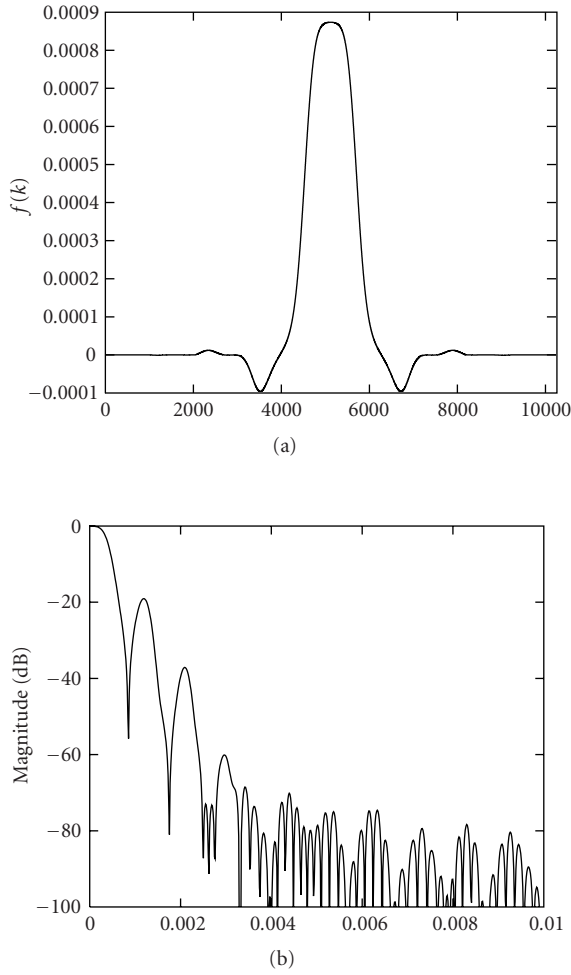


FIGURE 8: OFDM/QAM prototype filter maximizing the time-frequency localization; (a) filter coefficient and (b) frequency response, with  $M_0 = 4$ ,  $N_0 = 5$ ,  $m = 2$ ,  $M = 1024$ ,  $L = 10240$ ,  $\xi = 0.8034350$ .

Matlab function and we assume a perfect knowledge of the channel state at reception. Our simulation results include all the OFDM/QAM solutions depicted from Figures 3 to 8. They are compared to conventional OFDM systems with cyclic prefix (CP) leading to similar spectral efficiencies, that is, the ones corresponding either to an oversampling ratio such that  $r = 3/2$  or  $5/4$ . Figures 9 and 10 represent the mean square error (MSE), that is,  $E\{|\hat{c}_{m,n} - \tilde{c}_{m,n}|^2\}$ , versus the maximum Doppler frequency (using normalized frequencies). For each oversampling ratio, using optimized pulses can lead to a reduction of the mean square error.

When normalized Doppler frequency is less than  $10^{-3.7} = 2.10^{-4}$ , simulations results (see Figures 9 and 10) show that time-frequency optimized pulses achieve better mean square error than pulses minimizing out-of-band energy. Beyond this value, the channel fades too slowly to exhibit a difference between the pulses. Moreover, for any normalized Doppler frequency, both criteria allow it to improve OFDM with pre-cyclic.

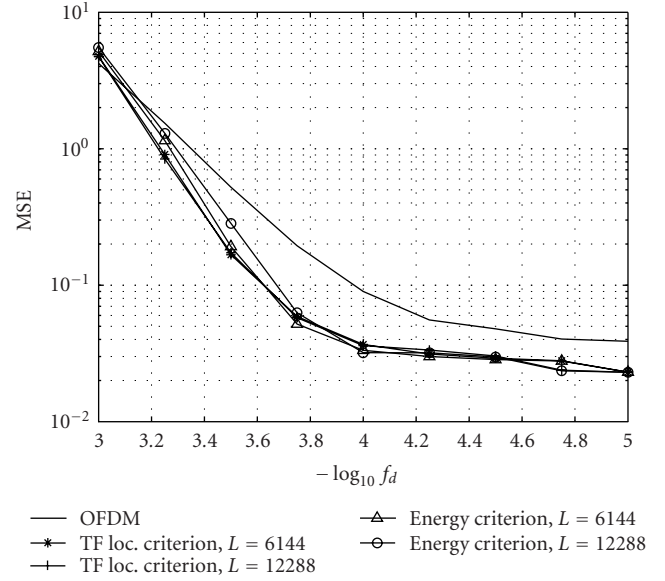


FIGURE 9: Comparison of an optimized pulse with CP-OFDM, for  $M = 1024$  and  $N = 1536$ .

It is worthwhile noting that CP-OFDM does not reach the same limit as optimized pulses when the channel is almost constant (i.e.,  $f_a$  tends to 0). This is due to the fact that introducing a cyclic prefix implies a loss of energy per symbol equal to  $N/M$ . But at the contrary, oversampling allows it to divide the energy per symbol by  $N/M$  (cf. [16]), at the price of a loss of spectral efficiency. That is also why pulses optimized with an oversampling ratio equal to  $r = 5/4$  (cf. Figure 10) provide a greater MSE than those optimized for  $r = 3/2$  (cf. Figure 9), when  $f_a$  tends to 0.

## 7. CONCLUSION

We have presented a theoretical analysis of oversampled DFT-modulated transmultiplexers and filter banks. The perfect reconstruction (PR) conditions have been established in the polyphase domain for a pair of biorthogonal prototype filters and considering a rational oversampling ratio. A decomposition theorem has been proposed that allows it to split the initial system of PR equations, that can be huge, into small independent subsystems of equations. In the orthogonal case, it has been shown that these subsystems can be solved thanks to an appropriate angular parametrization. As these parameters present some smoothness properties with respect to a polyphase component index, we could, as in [22] for critically decimated filter banks, use our compact representation to significantly and efficiently reduce the number of parameters to optimize. Using two different design criteria, the minimization of the out-of-band energy and the maximization of the time-frequency localization, we have provided various design examples corresponding to systems with 1024 carriers (or subbands) and oversampling ratios equal to  $3/2$  and  $5/4$ . On the application side, it has been



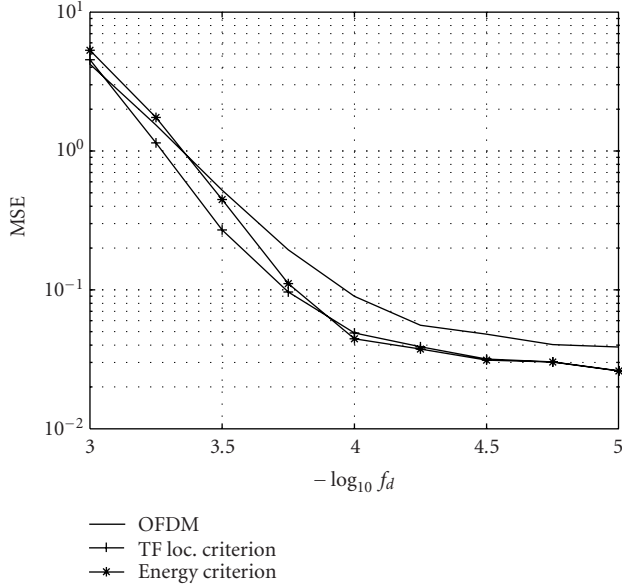


FIGURE 10: Comparison of an optimized pulse with CP-OFDM, for  $M = 1024$  and  $N = 1280$ .

shown that these oversampled OFDM systems could outperform the conventional OFDM in the case of a transmission over a frequency-dispersive flat fading channel. However, further theoretical and experimental studies will be necessary to make oversampled OFDM systems still more attractive. Thus, we are now investigating a new parametrization technique in order to directly get the parametrical solutions of maximum dimensions for oversampling ratios still closer to 1. Reference [19] also suggests some other possible improvements that could perhaps be adapted to our filter bank approach. In this context, this could also result, by the introduction of nonrectangular time-frequency lattices, in better time-frequency localization values.

## APPENDIX

Let  $\mathcal{S}$  be an algebraic system of equations with  $n$  variables  $x_1, x_2, \dots, x_n$  and  $f : \mathcal{O} \subset \mathbb{R}^k \rightarrow \mathbb{R}^n$  one application defined over a dense subset  $\mathcal{O}$  of  $\mathbb{R}^k$  with  $f = (f_1, f_2, \dots, f_n)$ , so that  $x_1 = f_1(\theta_1, \theta_2, \dots, \theta_k), \dots, x_n = f_n(\theta_1, \theta_2, \dots, \theta_k)$  is a solution of  $\mathcal{S}$  for every  $(\theta_1, \theta_2, \dots, \theta_k)$  in  $\mathcal{O}$ .

If the functions  $f_i$  are polynomials in  $\cos \theta_j$  and  $\sin \theta_j$ ,  $j = 1, \dots, k$ , with integer coefficients, that is also the case for their first-order partial derivatives.

In this case, the set  $f(\mathcal{O})$  is an open space of an algebraic subvariety of  $\mathbb{R}^n$ . On a point  $(\theta_1, \theta_2, \dots, \theta_k)$ , the dimension of  $f$  is defined by the rank of the  $(n, k)$  Jacobian matrix  $J$  given by

$$J_{i,j} = \frac{\partial f_i}{\partial \theta_j}(\theta_1, \theta_2, \dots, \theta_k), \quad i = 1, \dots, n, \quad j = 1, \dots, k. \quad (\text{A.1})$$

However, in general, a formal or numerical computation of the rank of  $J$  is hardly feasible. So, another approach is proposed here to compute the dimension corresponding to this parametrical representation of a solution. Excepting a set with null measure in the open set  $\mathcal{O}$ , the rank of the Jacobian matrix is equal to its maximum value on  $\mathcal{O}$ , which is called the dimension or the rank of  $f$ . Thus, we may restrict ourselves to angular parameters values  $\theta_j$ ,  $j = 1, \dots, k$ , so that  $\cos \theta_j$  and  $\sin \theta_j$  are rational numbers. The evaluation of the polynomials in  $\cos \theta_j$  and  $\sin \theta_j$  occurring in the computation of the rank of the Jacobian matrix may then be done exactly. Our probabilistic approach therefore consists of a computation of the dimension using one or several random selections of the  $\cos \theta_j$  and  $\sin \theta_j$ . If a parametrical solution has a dimension equal to the maximum dimension obtained considering a set of parametrical solutions, we say that this solution is of maximum dimension or maximum rank in this set.

## ACKNOWLEDGMENTS

Part of this work was carried out when Dr. C. Siclet was at France Télécom. This work is also partly supported by the European Network of Excellence NEWCOM. The authors would like to thank the anonymous reviewers for valuable comments that have led to improvements in this paper.

## REFERENCES

- [1] H. Bölcskei, F. Hlawatsch, and H. G. Feichtinger, "Frame-theoretic analysis of oversampled filter banks," *IEEE Transactions on Signal Processing*, vol. 46, no. 12, pp. 3256–3268, 1998.
- [2] R. Hleiss, P. Duhamel, and M. Charbit, "Oversampled OFDM systems," in *Proceedings of 13th IEEE International Conference on Digital Signal Processing (DSP '97)*, vol. 1, pp. 329–332, Santorini, Greece, July 1997.
- [3] R. Hleiss, *Conception et égalisation de nouvelles structures de modulations multiporteuses*, Ph.D. thesis, École Nationale Supérieure des Télécommunications de Paris (ENSTP), Paris, France, 2000.
- [4] Y.-P. Lin and S.-M. Phoong, "ISI-free FIR filterbank transceivers for frequency-selective channels," *IEEE Transactions on Signal Processing*, vol. 49, no. 11, pp. 2648–2658, 2001.
- [5] C. Siclet, P. Siohan, and D. Pinchon, "Analysis and design of OFDM/QAM and BFDQ/QAM oversampled orthogonal and biorthogonal multicarrier modulations," in *Proceedings of IEEE International Conference on Acoustics, Speech, and Signal Processing (ICASSP '02)*, vol. 4, pp. IV-4181, Orlando, Fla, USA, May 2002.
- [6] S.-M. Phoong, Y. Chang, and C.-Y. Chen, "DFT-modulated filterbank transceivers for multipath fading channels," *IEEE Transactions on Signal Processing*, vol. 53, no. 1, pp. 182–192, 2005.
- [7] M. Vetterli, "Perfect transmultiplexers," in *Proceedings of IEEE International Conference on Acoustics, Speech, and Signal Processing (ICASSP '86)*, vol. 11, pp. 2567–2570, Tokyo, Japan, April 1986.
- [8] H. Bölcskei, "Efficient design of pulse-shaping filters for OFDM systems," in *Wavelet Applications in Signal and Image Processing VII*, vol. 3813 of *Proceedings of SPIE*, pp. 625–636, Denver, Colo, USA, July 1999.

- [9] M. Vetterli, "Filter banks allowing perfect reconstruction," *Signal Processing*, vol. 10, no. 3, pp. 219–244, 1986.
- [10] J. Louveaux, *Filter bank based multicarrier modulation for xDSL transmission*, Ph.D. thesis, Laboratoire de Télécommunications et Télédetection, Université Catholique de Louvain (UCL), Louvain-la-Neuve, Belgium, May 2000.
- [11] B. Le Floch, M. Alard, and C. Berrou, "Coded orthogonal frequency division multiplex," *Proceedings of IEEE*, vol. 83, no. 6, pp. 982–996, 1995.
- [12] A. Vahlin and N. Holte, "Optimal finite duration pulses for OFDM," *IEEE Transactions on Communications*, vol. 44, no. 1, pp. 10–14, 1996.
- [13] R. Haas and J.-C. Belfiore, "A time-frequency well-localized pulse for multiple carrier transmission," *Wireless Personal Communications*, vol. 5, no. 1, pp. 1–18, 1997.
- [14] H. Bölcskei, "Orthogonal frequency division multiplexing based on offset-QAM," in *Advances in Gabor Analysis*, pp. 321–352, Birkhäuser, Boston, Mass, USA, 2002.
- [15] P. Siohan, C. Siclet, and N. Lacaille, "Analysis and design of OFDM/OQAM systems based on filterbank theory," *IEEE Transactions on Signal Processing*, vol. 50, no. 5, pp. 1170–1183, 2002.
- [16] C. Siclet, *Application de la théorie des bancs de filtres à l'analyse et à la conception de modulations multiporteuses orthogonales et biorthogonales*, Ph.D. thesis, Université de Rennes I (URI), Rennes, France, 2002.
- [17] W. Kozek and A. F. Molisch, "Nonorthogonal pulseshapes for multicarrier communications in doubly dispersive channels," *IEEE Journal on Selected Areas in Communications*, vol. 16, no. 8, pp. 1579–1589, 1998.
- [18] D. Schafhuber, G. Matz, and F. Hlawatsch, "Pulse-shaping OFDM/BFDM systems for time-varying channels: ISI/ICI analysis, optimal pulse design, and efficient implementation," in *Proceedings of 13th IEEE International Symposium on Personal, Indoor and Mobile Radio Communications (PIMRC '02)*, vol. 3, pp. 1012–1016, Lisbon, Portugal, September 2002.
- [19] T. Strohmer and S. Beaver, "Optimal OFDM design for time-frequency dispersive channels," *IEEE Transactions on Communications*, vol. 51, no. 7, pp. 1111–1122, 2003.
- [20] Z. Cvetković and M. Vetterli, "Tight Weyl-Heisenberg frames in  $L^2(\mathbf{Z})$ ," *IEEE Transactions on Signal Processing*, vol. 46, no. 5, pp. 1256–1259, 1998.
- [21] D. Pinchon, C. Siclet, and P. Siohan, "A design technique for oversampled modulated filter banks and OFDM/QAM modulations," in *Proceedings of 11th International Conference on Telecommunications (ICT '04)*, pp. 578–588, Fortaleza, Brazil, August 2004.
- [22] D. Pinchon, P. Siohan, and C. Siclet, "Design techniques for orthogonal modulated filter banks based on a compact representation," *IEEE Transactions on Signal Processing*, vol. 52, no. 6, pp. 1682–1692, 2004.
- [23] H. Bölcskei and F. Hlawatsch, "Oversampled modulated filter banks," in *Gabor Analysis: Theory, Algorithms, and Applications*, chapter 9, pp. 295–322, Birkhäuser, Boston, Mass, USA, 1998.
- [24] P. P. Vaidyanathan, *Multirate Systems and Filter Banks*, Prentice-Hall, Englewoods Cliffs, NJ, USA, 1993.
- [25] T. Strohmer, "Finite and infinite-dimensional models for oversampled filter banks," in *Modern Sampling Theory: Mathematics and Applications*, pp. 297–320, Birkhäuser, Boston, Mass, USA, 2000.
- [26] M. I. Doroslovački, "Product of second moments in time and frequency for discrete-time signals and the uncertainty limit," *Signal Processing*, vol. 67, no. 1, pp. 59–76, 1998.
- [27] W. C. Jakes, Ed., *Microwave Mobile Communications*, Wiley-IEEE Press, Piscataway, NJ, USA, 2nd edition, 1994.

**Cyrille Siclet** was born in Champigny-sur-Marne, France, in September 1976. He received the Engineer degree in telecommunications from the École Nationale Supérieure des Télécommunications (ENST) de Bretagne (1999), the M.S. degree (DEA) and the Ph.D. degree from the University of Rennes, France, in 1999 and 2002, respectively. He had been working for France Télécom R&D, Rennes (1999–2002), for the Catholic University of Louvain (UCL), Belgium (2002–2003), for the Research Center in Automatic Control of Nancy (CRAN), France (2003–2004), and he is currently working at the Image and Signal Processing Laboratory (LIS), Grenoble, France.



**Pierre Siohan** was born in Camlez, France, in October 1949. He received the Ph.D. degree from the École Nationale Supérieure des Télécommunications (ENST), Paris, France, in 1989, and the Habilitation degree from the University of Rennes, Rennes, France, in 1995. In 1977, he joined the Centre Commun d'Études de Télédiffusion et Télécommunications (CCETT), Rennes, where his activities were first concerned with the communication theory and its application to the design of broadcasting systems. Between 1984 and 1997, he was in charge of the Mathematical and Signal Processing Group. Since September 1997, he has been an Expert Member in the R&D Division of France Télécom working in the Broadband Wireless Access Laboratory. From September 2001 to September 2003, he took a two-year sabbatical leave, being Directeur de Recherche with the Institut National de Recherche en Informatique et Automatique (INRIA), Rennes. His current research interests are in the areas of filter bank design for communication systems, joint source-channel coding, and distributed source coding.



**Didier Pinchon** was born in Chaumont-en-Vexin, France, in February 1949. After studying at École Nationale Supérieure de Saint-Cloud, France, he joined the Centre National de Recherche Scientifique (CNRS), Paris, France, as a Researcher, where he received the State Thesis degree in 1979 for various contributions in ergodic theory. From 1986 to 1990, he turned his interest to computer algebra applications. He was recruited by IBM France to lead a research group in this area at the IBM France Scientific Center, Paris. He returned to CNRS in 1990. He is currently working in the Mathematics for Industry and Physics Laboratory, Toulouse, France, where he is involved with computer algebra applications, mainly in signal processing, queues theory, and partial differential equations.

